Chapter 13

Small Strain Nonlinearity

TABLE OF CONTENTS

Chapter 13

Small Strain Nonlinearity

13.1 Introduction

In the previous chapter, in the models with pressure dependent stiffness, the shear modulus G was either constant or increased with the mean effective stress. These models used to describe the pre-yielding deviatoric behaviour of soils in standard triaxial compression tests reasonably well. The problem was that the corresponding numerical models considerably over-predicted displacements in many boundary value problems. In late 1980s this discrepancy lead researchers at Imperial College, London (e.g., Burland, 1989), to an idea to conduct laboratory tests with strains measured locally on the sample, as opposed to the external strain measurements in standard triaxial tests (Figure 13.1a). When plotted in a wide strain range (Figure 13.1b), the deviatoric stress-strain curves of the two tests do not differ that much. The curve for the local strain test (dashed line) goes slightly higher, but this does not affect the pre-yielding secant shear modulus G significantly. A different picture is observed when we zoom (Figure 13.1c) into the area of very small strains (up to 0.01-0.1%). While the externally measured stress-strain test curve (solid line) is almost linear, the locally measured stress-strain curve proves to be highly non-linear, with the initial tangent shear modulus G_0 almost an order of magnitude higher than the pre-yielding secant shear modulus G. Another important discovery was that even at the very small strains the stress-strain behaviour is not entirely reversible, i.e. it exhibits some very small permanent strains in a closed loading cycle (Figure 13.1c).

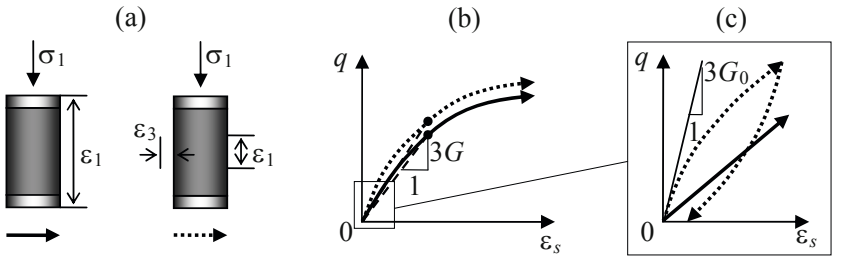

Figure 13.1 External vs. local deformation measurements in a triaxial test: (a) schematic setup; (b) deviatoric stress-strain curves; (c) zoom into small strains.

A.M. Puzrin, *Constitutive Modelling in Geomechanics,*
DOI 10.1007/978-3-642-27395-7_13, © Springer-Verlag Berlin Heidelberg 2012

Why is this high stiffness small strain behaviour so important? The reality is that in many practical geotechnical problems only a relatively small volume of soil experiences large deformations. The strains in the remaining part are very small. But to calculate displacements, these small strains are integrated over the large area and their overall contribution can be quite significant. Therefore, underestimation of the soil stiffness at small strains in standard tests results (for the same stress level) in overestimating the strains and displacements in geotechnical boundary value problems.

The new understanding of the highly non-linear nature of the small strain behaviour of soils obtained from the local deformation measurement tests allowed for this problem to be solved. Provided, of course, that this non-linear behaviour is properly modelled.

13.2 Non-linear models of the small-strain behaviour

In this section we are going to consider a number of analytical functions for curve-fitting the deviatoric stress-strain behaviour of soils at small strains. What are the requirements this function should satisfy?

First of all it should be simple and contain a minimum number of parameters. These parameters should have a clear physical meaning and be easy to derive from standard lab tests. Finally, most importantly, the function should provide a good fit to the experimental deviatoric stress-strain curves. And this is exactly the catch: when our "elegant" function is not sufficiently accurate, we "modify" it by adding parameters, they loose their physical meaning, become difficult to derive, etc.. And this may still not be sufficient, if the intrinsic shape of the function is not the proper one. The best known "victim" of such modifications is the hyperbolic function, described below.

There are also some mathematical conditions the curve-fitting function should satisfy, but in order to formulate them, we first introduce a normalized deviatoric stress-strain space.

13.2.1 Normalized pre-yielding behaviour

The curve-fitting function does not necessarily have to fit the deviatoric stress-strain curve all the way up to the yield stress q_y, because the high non-linearity occurs normally at rather small strains. After a certain limiting deviator stress q_L and up to the yield stress q_y, the stress strain curve can be often well approximated by a straight line with inclination $3G_L$, corresponding to the tangent shear modulus G_L at the limiting stress q_L (Figure 13.2a). In this case an analytical function has to simulate the soil behaviour up to limiting deviator stress q_L (corresponding to the limiting shear strain ε_{sL}) only. The following normalisation of the curve within the above limits was found to be very convenient (Figure 13.2b):

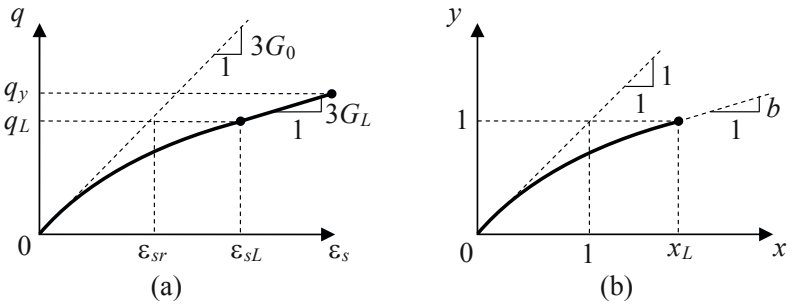

Figure 13.2 Deviatoric stress-strain curve: (a) true; (b) normalised.

$$y = \frac{q}{q_L}; \qquad x = \frac{\varepsilon_s}{\varepsilon_{sr}}; \qquad \varepsilon_{sr} = \frac{q_L}{3G_0}; \qquad x_L = \frac{\varepsilon_{sL}}{\varepsilon_{sr}}, \tag{13.1}$$

where y and x are the normalized deviator stress and strain, respectively; G_0 is the initial tangent shear modulus; x_L is the normalized limiting shear strain.

It follows, that

$$\frac{dy}{dx} = \frac{1}{3G_0}\frac{dq}{d\varepsilon_s} = \frac{G_t(x)}{G_0} \tag{13.2}$$

i.e., the tangent shear modulus in the normalized space is equal to the true tangent shear modulus G_t normalized by the initial modulus G_0. As a result, the normalized analytical curve-fitting function has to satisfy the following conditions at the end points of the fitting interval (Figure 13.2b):

$$x = 0; \qquad y = 0; \qquad \frac{dy}{dx} = 1, \tag{13.3}$$

$$x = x_L; \quad y = 1; \qquad \frac{dy}{dx} = b = \frac{G_L}{G_0}. \tag{13.4}$$

Let us now consider some popular normalized curve-fitting functions.

13.2.2 The hyperbolic function

The hyperbolic model was proposed for modelling soil behaviour by Konder (1963). In terms of simplicity it is the absolute champion – in the normalised form it does not have any parameters:

$$y = \frac{x}{1+x} \tag{13.5}$$

Of course, there is a price to pay – while conditions (13.3) are fully satisfied, conditions (13.4) are not. Furthermore $y = 1$ is reached only at the infinite strain $x = \infty$, where $dy/dx = 0$, i.e. the material is slowly approaching failure (Figure 13.3a). This means, that this function can only be applied in the full range of strains with $q_L = q_f$, i.e. the limiting deviator stress is equal to the failure stress (shear strength). In order to be able to apply this function for modelling pre-yielding behaviour, it has to be slightly modified:

$$y = \frac{x}{1+\alpha x}; \qquad \frac{dy}{dx} = \frac{1}{(1+\alpha x)^2}, \tag{13.6}$$

where an additional parameter

$$\alpha = \frac{x_L - 1}{x_L} \tag{13.7}$$

is introduced to satisfy the first condition (13.4). Example of this modified hyperbolic curve for $x_L = 5$ is given in Figure 13.3b by the dotted line. Further modifications are needed in order to also satisfy the second condition (13.4), but these are already too cumbersome and it is better to use other functions, which are designed to satisfy all these conditions, e.g. the Ramberg-Osgood function.

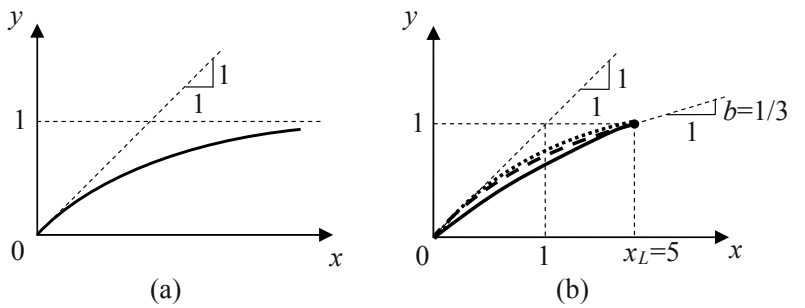

Figure 13.3 Normalized curve fitting functions: (a) original hyperbolic; (b) the modified hyperbolic, Ramberg-Osgood and logarithmic for $x_L = 5$, $b = 1/3$.

13.2.3 The Ramberg-Osgood function

The Ramberg-Osgood function was proposed by Ramberg and Osgood (1943):

$$x = y + \alpha y^R; \qquad \frac{dy}{dx} = \frac{1}{1 + \alpha R y^{R-1}}, \tag{13.8}$$

where parameters

$$\alpha = x_L - 1; \qquad R = \frac{1-b}{(x_L - 1)b} \tag{13.9}$$

are chosen to satisfy both conditions (13.3) and (13.4) in full. Example of this modified hyperbolic curve for $x_L = 5$ and $b = 1/3$ is given in Figure 13.3b by the dashed line.

The Ramberg-Osgood function was originally designed to model cyclic behaviour of soils, because parameter R could be alternatively found from the damping ratio of soil at the strain amplitude x_L. This will be explored more in detail in Section 13.3. For modelling the small strain behaviour of soils, however, the shape of the Ramberg-Osgood function is not as well fitting as that of some other functions, e.g. of the logarithmic function.

13.2.4 The logarithmic function

The logarithmic function was proposed by Puzrin and Burland (1996):

$$y = x - \alpha x \left[\ln(1 + x)\right]^R \tag{13.10}$$

with parameters

$$R = \frac{(1 + x_L)\ln(1 + x_L)}{(x_L - 1)}\left(\frac{1}{x_L} - b\right); \qquad \alpha = \frac{x_L - 1}{x_L\left[\ln(1 + x_L)\right]^R} \tag{13.11}$$

chosen to satisfy both conditions (13.3) and (13.4) in full. On top of that, however, this function has a correct shape - for realistic (for soils) values of x_L, it satisfies the following condition:

$$\left.\frac{d(y/x)}{dx}\right|_{x=0} = -\infty \tag{13.12}$$

which causes the curve to have a very high level of non-linearity at very small strains. This useful property proved to be instrumental in providing a very good fit to a large range of the small strain experimental data (Puzrin and Burland, 1996; 1998). Example of this modified hyperbolic curve for $x_L = 5$ and $b = 1/3$ is given in Figure 13.3b by the solid line.

13.3 Modelling irreversible small strain behaviour

Another important feature of the small strain behaviour of soils discovered in local deformation measurement tests is its irreversibility. The unloading and reloading stress-strain curves do not follow the initial loading curve (Figure 13.4a). Elastic behaviour, in principle, does not allow for plastic (permanent) strains, and the non-linear models presented above are elastic. This is less important when the soil element only experiences loading. But when certain stress reversals take place (e.g., in cyclic loading), modelling of the inelastic behaviour becomes an issue. In order to address this issue properly, the soil behaviour has to be considered within an elastic-plastic framework, as will be described in Chapter 20. Here we are going to present a simplified approach (sometimes called *deformational plasticity*) in which the small strain non-linear models are extended by assigning different loading, unloading and reloading shear moduli (G_L, G_U and G_R in Figure 13.4a, respectively). This can be done by adopting the so called Masing rules.

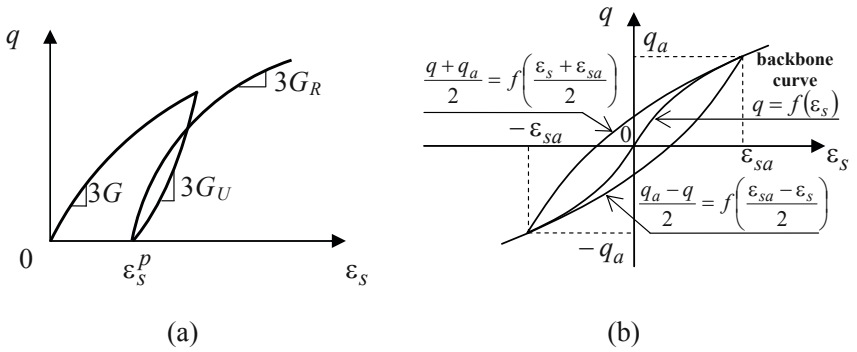

Figure 13.4 Irreversible stress-strain behaviour: (a) loading, unloading and reloading curves; (b) the Masing rules.

13.3.1 Masing rules

The Masing rules are a set of two original (Figure 13.4b) and two extended (e.g., Pyke, 1979) rules describing the one dimensional non-linear cyclic soil behaviour. Assume that the initial loading in a cyclic triaxial test can be described by the skeleton (or backbone) stress-strain curve (Figure 13.4b):

$$q = f(\varepsilon_s); \qquad 3G_t(\varepsilon_s) = \partial f(\varepsilon_s)/\partial \varepsilon_s \,. \tag{13.13}$$

This initial loading takes place up to the point A with deviator stress q_a, corresponding to the shear strain ε_{sa} ($q_a = f(\varepsilon_{sa})$), after which the sample

was unloaded to $-q_a$ and reloaded back to q_a (Figure 13.4b). The Masing rules can be then formulated as follows (Figure 13.4b):

1. The reloading curve can be obtained by scaling the backbone curve by a factor of 2 both along the q and ε axes. The unloading curve has the same shape as the reloading one, rotated by 180 degrees:

$$\frac{q_R + q_a}{2} = f\left(\frac{\varepsilon_s + \varepsilon_{sa}}{2}\right); \qquad \frac{q_a - q_U}{2} = f\left(\frac{\varepsilon_{sa} - \varepsilon_s}{2}\right). \tag{13.14}$$

   It follows, that the second stress reversal point B is located at $(-\varepsilon_a, -q_a)$, and the reloading curve meets the backbone curve again at the point $A(\varepsilon_a, q_a)$.
2. The initial tangent shear modulus G_{t0} after all the stress reversals is the same and is equal to the initial tangent shear modulus G_0 of the backbone curve (which is in fact the consequence of the Rule 1).

The first two rules (Masing, 1926) are sufficient to describe the regular cyclic loading (with the constant amplitude) only. For the general loading, two additional rules are necessary:

3. After the reloading/unloading curve meets the backbone curve again, further reloading/unloading continues along this backbone curve.
4. In general, every time a stress-strain curve meets a curve from a previous cycle, it will follow this previous curve.

The Masing rules appear to model the experimental irreversible small strain behaviour rather well (e.g., Puzrin and Shiran, 2000), provided the backbone curve $q = f(\varepsilon_s)$ is chosen properly.

13.3.2 Modelling cyclic and dynamic small strain behaviour

Non-linear stress-strain functions, in combination with the Masing rules, allow for a simplified equivalent-linear analysis of shear wave propagation in soils, which is an important component of many seismic and dynamic geotechnical problems. Soil parameters required by this equivalent-linear analysis for each value of the strain amplitude ε_{sa} are the secant shear modulus G_s and the damping ratio ξ, which can be expressed both in true and normalized stresses and strains:

$$G_s(\varepsilon_{sa}) = \frac{q_a}{3\varepsilon_{sa}} = \frac{f(\varepsilon_{sa})}{3\varepsilon_{sa}} \quad \text{or} \quad G_s(x_a) = \frac{y(x_a)}{x_a} G_0 \tag{13.15}$$

$$\xi(\varepsilon_{sa}) = \frac{2}{\pi}\left(\frac{2\int_0^{\varepsilon_{sa}} f(\varepsilon_s)d\varepsilon_s}{f(\varepsilon_{sa})\varepsilon_{sa}} - 1\right) \quad \text{or} \quad \xi(x_a) = \frac{2}{\pi}\left(\frac{2\int_0^{x_a} y(x)dx}{y(x_a)x_a} - 1\right) \tag{13.16}$$

The damping ratio is defined as the ratio between the W_D - energy dissipated in the closed cycle (equal to the area of the hysteresis loop in Figure 13.4b) and $4\pi W_s$, where $W_s = q_a\varepsilon_{sa}/2$ is the maximum strain energy of the equivalent elastic material.

For example, for the modified hyperbolic function (13.6) it gives:

$$G_s(x_a) = \frac{G_0}{1+\alpha x_a}; \qquad \xi(x_a) = \frac{4}{\pi}\left(1 - \frac{\ln(1+\alpha x_a)}{\alpha x_a}\right)\left(1 + \frac{1}{\alpha x_a}\right) - \frac{2}{\pi}. \tag{13.17}$$

For the Ramberg-Osgood function (13.8), which is more suitable for a stress controlled cyclic loading with the amplitude y_a, we obtain:

$$G_s(y_a) = \frac{G_0}{1+\alpha y_a^{R-1}}; \qquad \xi(y_a) = \frac{2}{\pi}\frac{\alpha y_a^{R-1}}{1+\alpha y_a^{R-1}}\frac{R-1}{R+1}. \tag{13.18}$$

Finally, for the logarithmic function (13.10):

$$G_s(x_a) = G_0\left(1 - \alpha\left[\ln(1+x_a)\right]^R\right)$$
$$\xi(x_a) = \frac{4}{\pi}\frac{\int_0^{x_a}\left(1 - \alpha\left[\ln(1+x)\right]^R\right)x dx}{\left(1 - \alpha\left[\ln(1+x_a)\right]^R\right)x_a^2} - \frac{2}{\pi} \tag{13.19}$$

The integral in the numerator of the last expression can be elaborated to a closed form using an exponential integral function. It is preferable, however, to calculate this integral numerically, except for some particular cases, when parameter R is an integer number.

13.3.3 Comparison between the non-linear models

Hyperbolic functions (13.5) and (13.6) are not really suitable for modelling dynamic behaviour of soils, because they cannot be fitted to the experimental damping ratio data $\xi(x_a)$, and they tend to overestimate the damping ratio at the medium to larger strains quite considerably.

An advantage of the Ramberg-Osgood function (13.8) is that one of its parameters, *R*, instead of being fitted using inclination *b* of the stress-strain curve at the normalised limiting strain x_L, can be calculated using equation (13.18) to provide the prescribed damping ratio $\xi_L = \xi(x_L)$ at this strain:

$$R = \frac{2(x_L - 1) - \pi x_L \xi_L}{2(x_L - 1) + \pi x_L \xi_L} \tag{13.20}$$

Nevertheless, at very small strains the Ramberg-Osgood model tends to under-predict the damping ratios, while at the medium strains to overpredict them (Puzrin and Shiran, 2000).

Finally, for the logarithmic function (13.10), its parameter R can also be defined via $\xi_L = \xi(x_L)$. However, generally, there is no need in that: the correct shape of the logarithmic function automatically guaranties a good fit to the experimental damping ratios both at small and medium strains (Puzrin and Shiran, 2000).

13.3.4 The proper theoretical framework

The proper way to model both the non-linearity and the irreversibility of the small strain behaviour is within the framework of the multiple surfaces kinematic hardening plasticity (e.g., Puzrin and Burland, 2000). In this case, the normalised non-linear deviatoric stress-strain curve is used to calibrate the hardening rule. Within this framework, all the four Masing rules for the irreversible cyclic behaviour are satisfied automatically! Chapter 20 of this book gives additional insight into this type of models.

13.4 Thermomechanics of the small strain non-linearity

Although the small strain non-linearity introduces a certain level of complexity into the constitutive modelling of soil, following some simple rules can prevent the corresponding models from violating the Laws of Thermodynamics.

13.4.1 Reversible non-linear behaviour and Thermomechanics

If the deviatoric behaviour is considered to be non-linear but reversible, it will always satisfy the First Law of Thermodynamics, provided the model parameters such as initial shear modulus G_0 and limiting stress q_L are both pressure independent. The bulk modulus $K(p')$ can still be pressure dependent. In this case, the Helmholz free energy function

$$f(\varepsilon_v, \varepsilon_s) = \frac{p'_0}{k} e^{k(\varepsilon_v - \varepsilon_{v0})} + \frac{q_L^2}{G_0} \int_0^{\varepsilon_s G_0 / q_L} y(x)dx \tag{13.21}$$

will produce the following decoupled volumetric and deviatoric behaviour:

$$p' = \frac{\partial f}{\partial \varepsilon_v} = p'_0 e^{k(\varepsilon_v - \varepsilon_{v0})}; \quad q = \frac{\partial f}{\partial \varepsilon_s} = q_L y\left(\frac{\varepsilon_s G_0}{q_L}\right), \tag{13.22}$$

where the first expression corresponds to the linear pressure dependency of

the bulk stiffness $K = \partial^2 f / \partial \varepsilon_v^2 = kp'$; while the second expression reproduces the chosen deviatoric non-linear stress-strain curve in the normalised form $y = y(x)$.

For the stress controlled behaviour, the corresponding Gibbs free energy function

$$g(p',q) = -\frac{p'}{k}\left(\ln\left(\frac{p'}{p'_0}\right)-1\right) - (p'-p'_0)\varepsilon_{v0} - \frac{q_L^2}{G_0}\int_0^{q/q_L} x(y)dy \tag{13.23}$$

will produce the same (but inverse) decoupled volumetric and deviatoric behaviour:

$$\varepsilon_v = -\frac{\partial g}{\partial p'} = \varepsilon_{v0} + \frac{1}{k}\ln\frac{p'}{p'_0}; \qquad \varepsilon_s = -\frac{\partial g}{\partial q} = \frac{q_L}{G_0}x\left(\frac{q}{q_L}\right) \tag{13.24}$$

For example, for the modified hyperbolic function (13.6), we obtain:

$$f(\varepsilon_v,\varepsilon_s) = \frac{p'_0}{k}e^{k(\varepsilon_v-\varepsilon_{v0})} + \frac{q_L^2}{G_0\alpha^2}\left(\alpha\varepsilon_s\frac{G_0}{q_L} - \ln\left(1+\alpha\varepsilon_s\frac{G_0}{q_L}\right)\right) \tag{13.25}$$

For the Ramberg-Osgood function (13.8), which is more suitable for a stress controlled loading, the Gibbs free energy is:

$$\begin{aligned} g(p',q) = &-\frac{p'}{k}\left(\ln\left(\frac{p'}{p'_0}\right)-1\right) - (p'-p'_0)\varepsilon_{v0} \\ &-\frac{q_L^2}{G_0}\left(\frac{1}{2}\left(\frac{q}{q_L}\right)^2 + \frac{\alpha}{R+1}\left(\frac{q}{q_L}\right)^{R+1}\right) \end{aligned} \tag{13.26}$$

Finally, for the logarithmic function (13.10), the Helmholz free energy is:

$$f(\varepsilon_v,\varepsilon_s) = \frac{p'_0}{k}e^{k(\varepsilon_v-\varepsilon_{v0})} + \frac{q_L^2}{G_0}\int_0^{\varepsilon_s G_0/q_L}\left(1-\alpha\left[\ln(1+x)\right]^R\right)xdx \tag{13.27}$$

The integral in the last expression can again be elaborated to a closed form using an exponential integral function.

In principle, also the reversible behaviour with shear stiffness dependent on pressure can be incorporated in a thermomechanically consistent way. For example, when the initial shear modulus G_0 and limiting stress q_L are both linearly dependent on the pressure:

$$G_0(p') = g_s p'; \qquad q_L = q_l p', \tag{13.28}$$

the following Gibbs free energy function:

$$g(p',q) = -\frac{p'}{k}\left(\ln\left(\frac{p'}{p'_0}\right)-1\right)-(p'-p'_0)\varepsilon_{v0}-\frac{q_l^2 p'}{g_s}\int_0^{q/q_l p'} x(y)dy \tag{13.29}$$

will produce the corresponding volumetric and deviatoric behaviour:

$$\varepsilon_v = -\frac{\partial g}{\partial p'} = \varepsilon_{v0}+\frac{1}{k}\ln\frac{p'}{p'_0}+\frac{q_l^2}{g_s}\int_0^{q/q_l p'} x(y)dy-\frac{q_l}{g_s p'}x\left(\frac{q}{q_l p'}\right) \tag{13.30}$$

$$\varepsilon_s = -\frac{\partial g}{\partial q} = \frac{q_l}{g_s}x\left(\frac{q}{q_l p'}\right) \tag{13.31}$$

In this model, there is a *volumetric-deviatoric coupling*, but on the isotropic axis $q=0$ the model degenerates into a simple form with the linear pressure dependency of the bulk stiffness $K = kp'$, while for the pure shear $p' = p'_0$, the model reproduces the chosen deviatoric non-linear stress-strain curve in the normalised form $x = x(y)$.

13.4.2 Irreversible non-linear behaviour and Thermomechanics

As mentioned above, the proper way to model both the non-linearity and the irreversibility of the small strain behaviour is within the framework of the multiple surfaces kinematic hardening plasticity. This framework can be made thermomechanically consistent by applying to it the principles of *Continuous Hyperplasticity* (e.g., Puzrin et al., 2001; Puzrin and Houlsby, 2006). In this case, the resulting models will satisfy both the First and the Second Laws of Thermodynamics. The following Part III of this book is in general devoted to modelling of irreversible soil behaviour and its thermomechanical consistency.

http://www.springer.com/978-3-642-27394-0

Constitutive Modelling in Geomechanics
Introduction
Puzrin, A.
2012, VIII, 312 p., Hardcover
ISBN: 978-3-642-27394-0